Colloid & Polymer Science Colloid Polym Sci 272:855–871 (1994)

Diffusiophoresis and electrophoresis of elliptic cylindrical particles

H. J. Keh and T. Y. Huang

Department of Chemical Engineering, National Taiwan University, Taipei, Taiwan, Republic of China

Abstract: An exact analysis is presented for the diffusiophoresis and electrophoresis of a rigid elliptic cylindrical particle in a uniform applied field oriented arbitrarily with respect to its axis. The range of the interaction between the solute species and the particle surface is assumed to be small relative to the minimum dimension of the particle, but the effect of polarization of the diffuse species in the thin particle-solute interaction layer is incorporated. To solve the conservative equations governing the system, a slip velocity of fluid and normal fluxes of solute species at the outer edge of the thin diffuse layer which balance convection and diffusion of the solute species along the particle surface are used as the boundary conditions for the fluid domain outside the diffuse layer. Expressions for the migration velocity of the particle are obtained in closed forms for the cases of diffusiophoresis in a nonionic solute concentration gradient, diffusiophoresis in a concentration gradient of symmetric electrolyte, and electrophoresis in an external electric field. An interesting feature is found that the diffusiophoretic or electrophoretic velocity of the particle decreases with the reduction of the maximum length of the particle in the direction of migration. Also, the average migration velocity for an ensemble of identical, noninteracting elliptic cylinders with random orientation distribution is obtained for each case considered.

Key words: Diffusiophoresis – electrophoresis – elliptic cylinder – thin but polarized diffuse layer

1. Introduction

Driving forces for transport of colloidal particles generally include concentration gradients of the particles themselves (diffusion), bulk velocities of the disperse medium (convection), and gravitational or centrifugal fields (sedimentation). Problems of the colloidal transport induced by these well-known driving forces have been treated extensively in the past. Another category of driving forces for the migration of colloidal particles, which has commanded less attention, involves a nonuniform imposed field (such as electrical potential, temperature, or solute concentration) that interacts with the surface of each particle. An excellent review summarizing the current state of knowledge concerning particle motions associated with this mechanism, known as "phoretic motions", is given by Anderson [1].

Perhaps the most familiar example of the various phoretic motions of colloids is electrophoresis in which an external electric field acts on the electrical double layer of a charged particle. The electrophoretic velocity $\underset{\sim}{U}_0$ of a single nonconducting particle suspended in an unbounded fluid is related to the applied electric field $\underset{\sim}{E}^\infty$ (which is constant) by the Smoluchowski equation [2, 3],

$$\underset{\sim}{U}_0 = \frac{\varepsilon\zeta}{4\pi\eta}\underset{\sim}{E}^\infty . \tag{1}$$

Here, $\varepsilon/4\pi$ is the fluid permittivity, η is the fluid viscosity, and ζ is the zeta potential associated with the particle surface.

Another example of phoretic motion is diffusiophoresis [3], which is the migration of a solid particle in response to the macroscopic concentration gradient of a molecular solute; the solute

can be nonionic or ionic. The particle moves toward or away from a region of higher solute concentration, depending on some long-range interactions between the solute molecules and the particle. In an immense solution with a constant solute concentration gradient ∇n^{∞}, the diffusiophoretic velocity of a particle is

$$\underset{\sim}{U}_0 = \frac{kT}{\eta} L^* K \nabla n^{\infty} \tag{2}$$

for the case of nonionic solute [4], and

$$\underset{\sim}{U}_0 = \frac{\varepsilon\zeta}{4\pi\eta}\frac{kT}{Ze}\left[\frac{D_2 - D_1}{D_2 + D_1} + \frac{4kT}{Ze\zeta}\ln\cosh\left(\frac{Ze\zeta}{4kT}\right)\right]\frac{\nabla n^{\infty}}{n^{\infty}(\underset{\sim}{0})} \tag{3}$$

for the case of symmetric electrolyte solute [5]. Here, L^* is a characteristic length for the range of particle-solute interactions, K is the Gibbs adsorption length characterizing the strength of the adsorption (K and L^* are defined by Eqs. (28a) and (28d)), $n^{\infty}(\underset{\sim}{0})$ is the macroscopic solute concentration measured at the particle center $\underset{\sim}{0}$ in the absence of the particle, D_1 and D_2 are the diffusion coefficients of the anion and cation respectively, Z is the absolute value of the valences of ions, e is the charge of a proton, k is the Boltzmann constant, and T is the absolute temperature.

Equations (1)–(3) indicate that the electrophoretic and diffusiophoretic velocities of a particle are independent of particle size and shape. However, their validity is based on the assumptions that the local radii of curvature of the particle are much larger than the thickness of the particle-solute interaction layer at the particle surface and the effect of polarization (relaxation effect) of the diffuse solute species in the interfacial layer due to the nonuniform "osmotic" flow is negligible. The subscript "0" of the particle velocity $\underset{\sim}{U}_0$ in Eqs. (1)–(3) emphasizes that these expressions are only valid in the limit of these assumptions. Recently, important advances have been made in the evaluation of the phoretic velocities of colloidal particles relaxing these assumptions.

Taking the double-layer distortion from equilibrium as a perturbation, O'Brien and White [6] obtained a numerical calculation for the electrophoretic velocity of a dielectric sphere of radius a which was applicable to arbitrary values of ζ and κa; κ^{-1} is the Debye screening length defined by

$$\kappa^{-1} = \left(\frac{\varepsilon kT}{8\pi e^2 I}\right)^{\frac{1}{2}}, \tag{4}$$

where I is the ionic strength in the bulk solution. On the other hand, Dukhin and Derjaguin [3] obtained an analytical expression for the electrophoretic mobility of a spherical particle with a thin but polarized double layer in a solution of symmetrically charged, binary electrolyte. Some approximate analytical and semi-empirical formulas for the electrophoretic mobility of a spherical particle in a symmetric electrolyte solution have also been developed by O'Brien and Hunter [7] and Ohshima et al. [8] for small but finite κa. O'Brien [9] extended these analyses to the case of electrophoretic motion of a sphere in a solution containing an arbitrary combination of electrolytes.

In general, the result for the electrophoretic velocity of a colloidal sphere with a thin but polarized double layer in a symmetric electrolyte solution can be analytically expressed as [10]

$$\underset{\sim}{U} = \frac{\varepsilon\zeta}{4\pi\eta}\underset{\sim}{E}^{\infty}\left[\frac{1}{3}(2 + c_1 + c_2) + \frac{4kT}{3Ze\zeta}(c_1 - c_2)\ln\cosh\left(\frac{Ze\zeta}{4kT}\right)\right], \tag{5}$$

with

$$c_1 = \frac{1}{2a^2\Delta}(a^2 + a\beta_{22} + 3a\beta_{12} - 2a\beta_{11} + 2\beta_{12}\beta_{21} - 2\beta_{11}\beta_{22}), \tag{6a}$$

$$c_2 = \frac{1}{2a^2\Delta}(a^2 + a\beta_{11} + 3a\beta_{21} - 2a\beta_{22} + 2\beta_{12}\beta_{21} - 2\beta_{11}\beta_{22}), \tag{6b}$$

and

$$\Delta = \frac{1}{a^2}(a^2 + a\beta_{11} + a\beta_{22} + \beta_{11}\beta_{22} - \beta_{12}\beta_{21}), \tag{7}$$

where β_{11}, β_{12}, β_{21}, and β_{22} are defined by Eqs. (41). If $|\zeta|$ is small and κa is large, the interaction between the diffuse counterions and the particle surface is weak and the polarization of the double

layer is also weak. In the limit of

$$(\kappa a)^{-1}\exp\left(\frac{Ze|\zeta|}{2kT}\right)\to 0\,, \tag{8}$$

$c_1 = c_2 = 0.5$ ($\beta_{11}/a = \beta_{12}/a = \beta_{21}/a = \beta_{22}/a = 0$), and Eq. (5) reduces to the Smoluchowski equation (1).

For the case of diffusiophoretic motion of a sphere with a thin but polarized interaction layer in a gradient of non-electrolyte solute, the following formula for the particle velocity has been analytically derived [11]:

$$\underset{\sim}{U} = \frac{kT}{\eta}L^*K\left[1+(1+vPe)\frac{K}{a}\right]^{-1}\nabla n^\infty\,, \tag{9}$$

where the definitions of v and Pe are given by Eqs. (28b) and (28c). For the case of a strongly adsorbing solute, the ratio K/a can be much greater than unity. In the limit of $K/a \to 0$ (weak adsorption), the polarization of the diffuse solute in the interfacial region vanishes and Eq. (9) reduces to Eq. (2).

On the other hand, Prieve and Roman [12] obtained a numerical solution of the diffusiophoretic velocity over a broad range of ζ and κa for a rigid insulating sphere in concentration gradients of symmetric electrolytes (KCl or NaCl) using the method of O'Brien and White [6]. Extending the analyses [3, 9, 10] for the electrophoresis of a spherical particle, Keh and Chen [13] recently obtained the following analytical expression for the diffusiophoretic velocity of a dielectric sphere with a thin polarized double layer in a symmetric electrolyte solution:

$$\underset{\sim}{U} = \frac{\varepsilon\zeta}{4\pi\eta}\frac{kT}{Ze}\frac{\nabla n^\infty}{n^\infty(\underset{\sim}{0})}\left[\frac{2}{3}\left(\frac{D_2-D_1}{D_2+D_1}+b_1-b_2\right)+\frac{8kT}{3Ze\zeta}\right.$$
$$\left.\times(1+b_1+b_2)\ln\cosh\left(\frac{Ze\zeta}{4kT}\right)\right]\,, \tag{10}$$

where

$$b_1 = \frac{D_2}{D_2+D_1}c_1 - \frac{3}{2a\Delta}\beta_{12}\,, \tag{11a}$$

$$b_2 = \frac{D_1}{D_2+D_1}c_2 - \frac{3}{2a\Delta}\beta_{21}\,, \tag{11b}$$

and c_1 and c_2 are defined by Eqs. (6). In the limiting situation as given in Eq. (8), Eq. (10) reduces to Eq. (3).

It could be found from Eqs. (5), (9), and (10) that the effect of polarization of the diffuse layer is to decrease the particle velocity. The reason for this consequence is that the transport of the solute inside the interaction region between the solute and the particle reduces the field along the particle surface.

The phoretic theories of nonspherical particles differ from those of spheres in that there is an orientational problem. In general, under polarized conditions, the phoretic mobility of a nonspherical particle is anisotropic and the velocity of the particle is no longer collinear with the applied field. The phoretic motions of a long circular cylinder with a thin but distorted particle-solute interaction layer were studied for the cases of electrophoresis [13–15] and diffusiophoresis [13]. A remarkable feature was found that the diffusiophoretic or electrophoretic velocity of the cylinder in a transversely-imposed field is exactly the same as the corresponding velocity of a rigid sphere with an equal radius. The phoretic motions of a spheroidal particle with a thin polarized diffuse layer have also been investigated for both cases of electrophoresis [16, 17] and diffusiophoresis [17].

It would be interesting to understand the effect of the form anisotropy of the normal cross-section of a long cylinder on its phoretic mobilities. In this paper we present a common analysis of the diffusiophoretic (in gradients of non-electrolytes or electrolytes) and electrophoretic motions of an elliptic cylindrical particle with a thin but polarized particle-solute interaction layer at the particle surface. We chose the elliptic cylinder as the model, because when the aspect ratio of its cross-sectional ellipse takes different values, the ellipse will have various forms, ranging from a circle to a line segment. The elliptic cylinder can be oriented arbitrarily with respect to the imposed field. The particle velocities are determined in closed forms as functions of relevant parameters for various cases.

2. Basic equations for phoretic motions

We first consider the diffusiophoretic or electrophoretic motion of a rigid particle of arbitrary shape in an unbounded liquid solution containing M chemical species (ionic or nonionic). The layer

of interaction between the solute species and the particle surface is assumed to be thin in comparison with the particle dimension. Hence, the fluid phase can be divided into two regions: an "inner" region defined as the interaction layer adjacent to the particle surface and an "outer" region defined as the remainder of the fluid.

In the outer region, the equations of conservation of the solute species and fluid momentum can be expressed by the Laplace equation

$$\nabla^2 \mu_m = 0, \quad m = 1, 2, \ldots, M , \tag{12}$$

and the Stokes equations

$$\eta \nabla^2 \underset{\sim}{v} - \nabla p = \underset{\sim}{0} , \tag{13}$$

$$\nabla \cdot \underset{\sim}{v} = 0 . \tag{14}$$

In Eq. (12), μ_m is the modified chemical potential energy of species m defined as

$$\mu_m = \mu_m^0 + kT \ln n_m + \Phi_m , \tag{15}$$

where μ_m^0 is a constant; n_m is the concentration of species m; Φ_m represents all kinds of potential energy resulting from van der Waals forces, electrical forces, etc., for the interaction between type-m species and the particle surface. In Eqs. (13) and (14), $\underset{\sim}{v}$ is the fluid velocity field and p is the dynamic pressure. For ionic species, the modified chemical potentials μ_m are also known as the electrochemical potentials [8].

The governing equations (12)–(14) in the outer region ought to satisfy the following boundary conditions at the particle surface (s_p^+) obtained by solving for the fluid velocity and the modified chemical potentials of the solute species in the inner region (balancing convection and diffusion of the solute species along the surface) and using a matching procedure to ensure a continuous solution in the whole fluid phase [9, 13]:

on S_p^+:

$$\underset{\sim}{n} \cdot \nabla \mu_m = - \sum_{i=1}^{M} \beta_{mi} \underset{\approx}{I} : \nabla_S \nabla_S \mu_i , \quad i = 1, 2, \ldots, M , \tag{16}$$

$$\underset{\sim}{v} = \underset{\sim}{U} + \underset{\sim}{\Omega} \times \underset{\sim}{r} + \underset{\sim}{v}_s , \tag{17}$$

with

$$\beta_{mi} = \delta_{mi} \int_0^\infty [\exp(-\Phi_m^0/kT) - 1] \, dy_n + \frac{kT}{\eta D_m} n_i^\infty \int_0^\infty [\exp(-\Phi_m^0/kT) - 1] \times \int_0^{y_n} \int_{y_n'}^\infty [\exp(-\Phi_i^0/kT) - 1] \, dy_n'' dy_n' dy_n \tag{18}$$

and

$$\underset{\sim}{v}_s = -\frac{1}{\eta} \sum_{m=1}^{M} \nabla_s \mu_m \int_0^\infty y_n [n_m^0 - n_m^\infty(\underset{\sim}{0})] \, dy_n . \tag{19}$$

In Eqs. (16)–(19), n_m^0 and Φ_m^0, functions of y_n, are the equilibrium concentration and potential energy, respectively, of species m; y_n is the distance measured from the particle surface along $\underset{\sim}{n}$, which is the unit vector outwardly normal to the surface; $n_m^\infty(\underset{\sim}{0})$ is the bulk concentration of species m measured at the particle center $\underset{\sim}{0}$ in the absence of the particle; $\underset{\sim}{r}$ is the position vector from the particle center; $\underset{\approx}{I}$ is the unit dyadic; $\nabla_s = (\underset{\approx}{I} - \underset{\sim}{n}\underset{\sim}{n}) \cdot \nabla$ represents the gradient operator along the particle surface; δ_{mi} denotes the Kronecker delta which is unity if i equals m, and zero otherwise; $\underset{\sim}{U}$ and $\underset{\sim}{\Omega}$ are the translational and angular velocities of the particle to be determined. Here, the term "surface" means outer limit of the thin interaction layer surrounding the particle. If the fluid is only slightly nonuniform in the undisturbed solute concentrations (n_m^∞) on the length scale of the particle dimension, the equilibrium concentration of any species is related to its equilibrium potential energy by the Boltzmann distribution

$$n_m^0 = n_m^\infty(\underset{\sim}{0}) \exp(-\Phi_m^0/kT) . \tag{20}$$

The modified chemical potentials far away from the particle approach the undisturbed values and the fluid is motionless there. Thus, μ_m and $\underset{\sim}{v}$ must obey

$$|\underset{\sim}{r}| \to \infty : \mu_m \to \mu_m^0 + kT \ln n_m^\infty + \Phi_m^\infty , \tag{21}$$

$$\underset{\sim}{v} \to \underset{\sim}{0} . \tag{22}$$

In Eq. (21), $\Phi_m^\infty = 0$ for the case of diffusiophoresis and $\nabla \Phi_m^\infty = -ez_m \underset{\sim}{E}^\infty$ for the case of electrophoresis, where z_m is the valence of type-m ions.

Because there is no effective external field exerted beyond the outer edge of the particle-solute interaction layer, the particle (plus its adjacent diffuse layer) is force and torque free. With this constraint, one can calculate the particle velocities $\underset{\sim}{U}$ and $\underset{\sim}{\Omega}$ after solving Eqs. (12)–(22) for the modified chemical potentials and the fluid velocity. The application of an external field to a nonspherical particle will in general give rise to a nonzero $\underset{\sim}{\Omega}$. For the motion of an elliptic cylinder, however, there can be no rotation due to the linearity of the governing equations (12)–(22) and the symmetry of the particle shape.

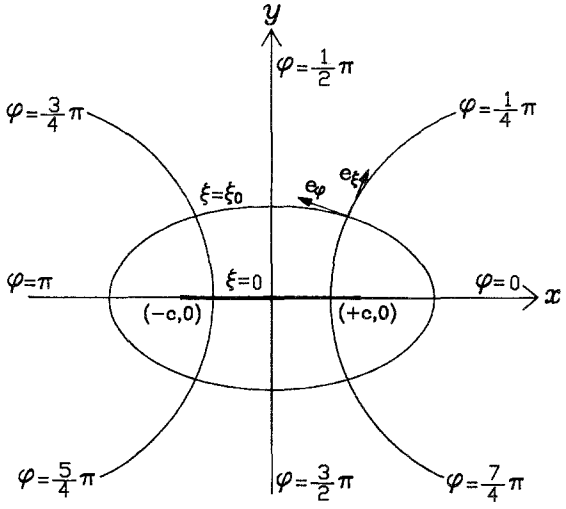

Fig. 1. The elliptic cylinder coordinate system

3. Diffusiophoresis in a nonelectrolyte solute gradient

In this section we consider the diffusiophoretic motion of an infinitely-long elliptic cylinder suspended in an unbounded solution of a nonelectrolyte solute ($M = 1$) with a constant concentration gradient ∇n^∞. The lengths of the major and minor semiaxes of the cross-sectional ellipse of the cylindrical particle are a and b, respectively. It is assumed that $a|\nabla n^\infty|/n^\infty(\underset{\sim}{0}) \ll 1$ and $L/b \ll 1$, where L is the characteristic thickness of the particle-solute interaction layer (which is approximately the molecular dimension of the solute). The interaction between a single solute molecule and the particle surface is described by the potential energy $\Phi(y_n)$, which decays to zero when $y_n/L \gg 1$.

To conveniently satisfy the boundary conditions at the particle surface, the elliptic cylinder coordinate system (ξ, φ, z), illustrated in Fig. 1, is utilized. This coordinate system is related to the rectangular coordinates (x, y, z) by the relation (in any plane z = constant) [18]

$$x = c\cosh\xi\cos\varphi\,, \tag{23a}$$

$$y = c\sinh\xi\sin\varphi\,, \tag{23b}$$

where $0 \le \xi < \infty$, $0 \le \varphi < 2\pi$, and c is a characteristic length which is positive. The family of curves in the xy plane characterized by the parameters ξ = constant are ellipses having their centers at the origin and their two foci at the points $(x = \pm c, y = 0)$. The lengths of the major and minor semiaxes of the ellipse $\xi = \xi_0$, which corresponds to the normal cross-section of the elliptic cylinder, are given by

$$a = c\cosh\xi_0\,, \tag{24a}$$

$$b = c\sinh\xi_0\,. \tag{24b}$$

Equations (23) show that when $\xi_0 = 0$ the ellipse is degenerate and corresponds to that segment of the x axis lying between the two foci. As $\xi_0 \to \infty$ the ellipse approaches a circle of infinite radius.

The solute gradient ∇n^∞ can be taken as a combination of the longitudinal component $(\nabla n^\infty)_z \underset{\sim}{e}_z$ and the transversal component $(\nabla n^\infty)_x \underset{\sim}{e}_x + (\nabla n^\infty)_y \underset{\sim}{e}_y$ with respect to the orientation of the elliptic cylinder, where $\underset{\sim}{e}_x$, $\underset{\sim}{e}_y$ and $\underset{\sim}{e}_z$ are the unit vectors in the Cartesian coordinate system. Thus, the general problem can be divided into two subproblems due to the linearity and they will be separately solved. The total diffusiophoretic velocity of the elliptic cylinder can be obtained by the vectorial addition of the two component results.

We first consider the diffusiophoretic motion of the elliptic cylinder due to the transverse component of the solute gradient, $(\nabla n^\infty)_x \underset{\sim}{e}_x + (\nabla n^\infty)_y \underset{\sim}{e}_y$. The modified chemical potential of the solute, μ, outside the particle-solute interaction layer is governed by the Laplace equation (12). A solution of it that satisfies the far-field boundary condition

(21) is

$$\mu = \mu^0 + kT\ln n^\infty(\underset{\sim}{0}) + \frac{kT(\nabla n^\infty)_x}{n^\infty(\underset{\sim}{0})}(x + Ae^{-\xi}\cos\varphi) + \frac{kT(\nabla n^\infty)_y}{n^\infty(\underset{\sim}{0})}(y + Be^{-\xi}\sin\varphi)\,, \tag{25}$$

where A and B are the unknown coefficients to be determined. At the cylinder surface (outer edge of the interaction layer) this solution obeys Eq. (16), which can be written as

$$\xi = \xi_0^+ : \frac{\partial\mu}{\partial\xi} = -\frac{\beta}{c}\frac{\partial}{\partial\varphi}\left[(\sinh^2\xi + \sin^2\varphi)^{-\frac{1}{2}}\frac{\partial\mu}{\partial\varphi}\right], \tag{26}$$

where

$$\beta = (1 + vPe)K\,, \tag{27}$$

with

$$K = \int_0^\infty [\exp(-\Phi(y_n)/kT) - 1]\,dy_n\,, \tag{28a}$$

$$v = (L^*K^2)^{-1}\int_0^\infty \left\{\int_{y_n}^\infty [\exp(-\Phi(y_n'')/kT) - 1]\,dy_n''\right\}^2 dy_n\,, \tag{28b}$$

$$Pe = \frac{kT}{\eta D}L^*K\,n^\infty(\underset{\sim}{0})\,, \tag{28c}$$

and

$$L^* = K^{-1}\int_0^\infty y_n[\exp(-\Phi(y_n)/kT) - 1]\,dy_n\,. \tag{28d}$$

Here, D is the solute diffusion coefficient, K is the Gibbs adsorption length, Pe is the Peclet number, and vPe accounts for the effect of convection on the solute distribution just outside the adsorption layer.

Substituting Eq. (25) into Eq. (26), one can find that

$$A = ce^{\xi_0}\sinh\xi_0\frac{\pi c - 2\beta\coth\xi_0\,G(\xi_0)}{\pi c + 2\beta G(\xi_0)}\,, \tag{29a}$$

and

$$B = ce^{\xi_0}\cosh\xi_0\frac{\pi c - 2\beta\tanh\xi_0\,H(\xi_0)}{\pi c + 2\beta H(\xi_0)}\,, \tag{29b}$$

where

$$G(\xi_0) = \int_{-1}^{1}\left(\frac{1-x^2}{\cosh^2\xi_0 - x^2}\right)^{\frac{1}{2}}dx = 2\cosh\xi_0[E(\mathrm{sech}\xi_0) - \tanh^2\xi_0 K(\mathrm{sech}\xi_0)] \tag{30a}$$

and

$$H(\xi_0) = \int_{-1}^{1}\left(\frac{1-x^2}{\sinh^2\xi_0 + x^2}\right)^{\frac{1}{2}}dx = 2\cosh\xi_0[K(\mathrm{sech}\xi_0) - E(\mathrm{sech}\xi_0)]\,. \tag{30b}$$

In Eqs. (30)

$$K(\alpha) = \int_0^{\pi/2}(1 - \alpha^2\sin^2\theta)^{-\frac{1}{2}}\,d\theta \tag{31a}$$

and

$$E(\alpha) = \int_0^{\pi/2}(1 - \alpha^2\sin^2\theta)^{\frac{1}{2}}\,d\theta\,, \tag{31b}$$

which are the complete elliptic integrals of the first kind and second kind, respectively [19].

Knowing the modified chemical potential distribution in the fluid phase, we can now take up the solution of the fluid velocity field. The fluid motion outside the particle-solute interaction layer is governed by the Stokes equations (13) and (14) and subject to the boundary conditions (from Eqs. (17) and (22))

$$\xi = \xi_0^+ : \underset{\sim}{v} = U_x\underset{\sim}{e}_x + U_y\underset{\sim}{e}_y - \underset{\sim}{e}_\varphi\frac{1}{\eta c}(\sinh^2\xi + \sin^2\varphi)^{-\frac{1}{2}} \times \frac{\partial\mu}{\partial\varphi}\int_0^\infty y_n[n^0 - n^\infty(\underset{\sim}{0})]\,dy_n \tag{32a}$$

and

$$\xi \to \infty : \underset{\sim}{v} \to \underset{\sim}{0}\,, \tag{32b}$$

where $\underset{\sim}{e}_\varphi$ is a unit vector in the elliptic cylinder coordinate system, and $U_x\underset{\sim}{e}_x + U_y\underset{\sim}{e}_y$ denotes the diffusiophoretic velocity of the cylinder in the transverse direction. In Eq. (32a), the integral equals $n^\infty(\underset{\sim}{0})L^*K$ by the definition of Eq. (28d) and the equilibrium relation (20), and $\partial\mu/\partial\varphi$ can be calculated from Eq. (25) with A and B determined by Eqs. (29). With the force-free constraint,

Table 1. The normalized diffusiophoretic mobilities of an elliptic cylinder in non-electrolyte concentration gradients in the transverse directions parallel to the major axis (x) and the minor axis (y)

β/a	β/b	$a/b = 1.1$		$a/b = 1.01$		$a/b = 1$
		U_x/U_{x0}	U_y/U_{y0}	U_x/U_{x0}	U_y/U_{y0}	U/U_0
0.01		0.9899	0.9894	0.9901	0.9900	0.9901
	0.01	0.9908	0.9903	0.9902	0.9901	
0.1		0.9072	0.9031	0.9089	0.9085	0.9091
	0.1	0.9149	0.9111	0.9097	0.9093	
0.5		0.6615	0.6508	0.6661	0.6650	0.6667
	0.5	0.6825	0.6721	0.6683	0.6672	
1		0.4943	0.4823	0.4994	0.4981	0.5000
	1	0.5181	0.5062	0.5019	0.5006	
2		0.3282	0.3178	0.3328	0.3317	0.3333
	2	0.3496	0.3388	0.3350	0.3339	
10		0.0890	0.0852	0.0907	0.0903	0.0909
	10	0.0971	0.0930	0.0915	0.0911	
100		0.0098	0.0092	0.0099	0.0098	0.0099
	100	0.0106	0.0101	0.0100	0.0099	

the fluid velocity field $\underset{\sim}{v}$ and the particle velocity components U_x and U_y can be obtained by solving Eqs. (13), (14), and (32).

It can be shown that the fluid motion outside the diffuse layer surrounding the elliptic cylinder can be described by a two-dimensional irrotational flow [20] with the Lagrangian stream function $\Psi(\xi, \varphi)$ expressed by

$$\Psi = c\, e^{-(\xi - \xi_0)}(-U_x \sinh\xi_0 \sin\varphi + U_y \cosh\xi_0 \cos\varphi)\,, \tag{33}$$

where the components of the diffusiophoretic velocity are given by

$$U_x = \frac{kT}{\eta} L^* K (\nabla n^\infty)_x \left[\frac{A}{c} e^{-2\xi_0} + e^{-\xi_0}\cosh\xi_0\right] \tag{34a}$$

and

$$U_y = \frac{kT}{\eta} L^* K (\nabla n^\infty)_y \left[\frac{B}{c} e^{-2\xi_0} + e^{-\xi_0}\sinh\xi_0\right]. \tag{34b}$$

As to the diffusiophoretic motion induced by the longitudinal component $(\nabla n^\infty)_z$ of the solute concentration gradient, there is no disturbance in the concentration and velocity fields caused by the curvature of the cylinder like in the above analysis for the transverse motion. The longitudinal velocity of the cylinder is given by Eq. (2),

$$U_z = \frac{kT}{\eta} L^* K (\nabla n^\infty)_z\,. \tag{35}$$

Note that, when the solute is weakly adsorbing, i.e., $K/b \ll 1$ or $\beta/b \to 0$, Eqs. (34) will also reduce to the simpler form of Eq. (2).

The overall diffusiophoretic velocity of the elliptic cylinder is the sum of the transversal and longitudinal contributions,

$$\underset{\sim}{U} = U_x \underset{\sim}{e}_x + U_y \underset{\sim}{e}_y + U_z \underset{\sim}{e}_z\,. \tag{36}$$

Thus, in general, the direction of the particle migration will not be parallel to the prescribed solute gradient.

Usually, experimental values of the phoretic velocity are average results. For an ensemble of long elliptic cylinders with random orientation, the average particle velocity (aligned with the direction of ∇n^∞) is obtained by averaging the transversal and longitudinal mobilities,

$$\underset{\sim}{U}_{\text{av}} = \frac{1}{3}\left[\frac{U_x}{(\nabla n^\infty)_x} + \frac{U_y}{(\nabla n^\infty)_y} + \frac{U_z}{(\nabla n^\infty)_z}\right]\nabla n^\infty\,. \tag{37}$$

It is expected that the average velocity would be smaller for an ensemble of cylindrical particles of finite length, for which the effect of the diffuse-layer relaxation on U_z appears.

The coefficients A and B in Eqs. (34) have been calculated for various values of the aspect ratio

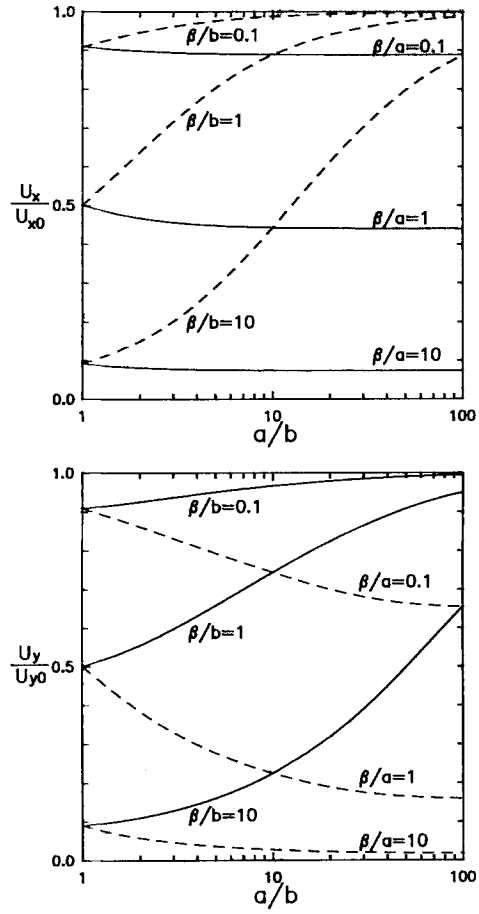

Fig. 2. Plots of the normalized diffusiophoretic mobilities of an elliptic cylindrical particle in a nonelectrolyte solution versus the aspect ratio for various values of the relaxation parameter: a) migration along the x-axis; b) migration along the y-axis

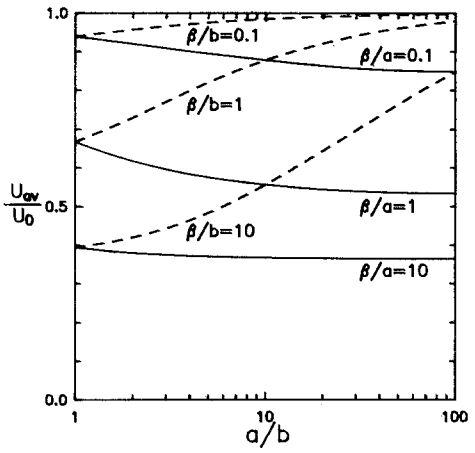

Fig. 3. Plots of the normalized average diffusiophoretic mobility in a dilute suspension of identical elliptic cylinders with nonelectrolyte concentration gradient versus the aspect ratio for various values of the relaxation parameter

a/b and the relaxation parameter β/a (or β/b, which indicates the strength of the solute adsorption to the particle surface). Numerical results of U_x and U_y for a transversely-diffusiophoretic elliptic cylinder with aspect ratio approaching unity ($a/b = 1.1$ and 1.01) are presented in Table 1 for various values of β/a and β/b. The magnitudes of the diffusiophoretic velocities are normalized by the corresponding values with negligible effect of the diffuse-layer polarization, given by (from Eq. (2))

$$U_{x0} = \frac{kT}{\eta} L^* K (\nabla n^\infty)_x \,, \tag{38a}$$

$$U_{y0} = \frac{kT}{\eta} L^* K (\nabla n^\infty)_y \,. \tag{38b}$$

The exact solutions of the normalized diffusiophoretic velocity of an infinitely-long circular cylinder (with $a/b = 1$) resulted from Eq. (9) and are also listed in the last column of Table 1 for comparison. It can be seen that our results for the elliptic cylinder with $a/b \to 1$ agree very well in tendency with the exact values for the circular cylinder.

An interesting feature is evident in Table 1: the normalized velocity U_x/U_{x0} is a much less sensitive function of the aspect ratio a/b for a fixed value of β/a than for a fixed value of β/b, while U_y/U_{y0} is a much less sensitive function of a/b for a given β/b than a given β/a. Namely, the maximum length of the particle in the direction of diffusiophoresis is the major factor of the particle dimension influencing the magnitude of the diffusiophoretic velocity. In general, the particle velocity decreases with the decrease of this length. This behavior is consistent with the observation in the phoretic motions of a spheroid [17].

The normalized velocities U_x/U_{x0} and U_y/U_{y0} of the elliptic cylinder as a function of the aspect ratio a/b (in the range from 1 to 10) are plotted in Figs. 2a and 2b, respectively. Three constant values, 0.1, 1 and 10, are chosen for the parameter β/a or β/b in these curves. Again, these curves demonstrate that U_x/U_{x0} does not vary too much with a/b for a given β/a and U_y/U_{y0} is a less sensitive function of a/b (when a/b is not large) for a fixed β/b than for a fixed β/a. These normalized

velocities are monotonic decreasing functions of a/b for a given value of β/a and are monotonic increasing functions of a/b for a given value of β/b. It can be seen from Table 1 and Figs. 2a and 2b that the migration velocity of the particle decreases monotonically with the increase of the relaxation parameter β/a or β/b.

The average diffusiophoretic velocity in a dilute suspension of identical elliptic cylinders can be evaluated using Eq. (37), and the numerical results of its normalized magnitude for three different values of β/a and β/b are plotted versus a/b in Fig. 3. Again, this average velocity is a monotonic decreasing (or increasing) function of a/b for a fixed parameter β/a (or β/b). In general, U_{av}/U_0 varies less sensitively with a/b for a given value of β/a than for a given value of β/b.

4. Diffusiophoresis in a concentration gradient of symmetric electrolytes

We now consider the diffusiophoretic motion of a uniformly-charged elliptic cylinder when immersed into a solution of symmetrically charged, binary electrolyte ($M = 2$) with a constant concentration gradient $\nabla n^\infty (n_1^\infty = n_2^\infty = n^\infty$, where subscripts 1 and 2 refer to the anion and cation respectively). Again, we assume $a|\nabla n^\infty|/n^\infty(\underset{\sim}{0}) \ll 1$. The electrical double layer is assumed to be much thinner than the particle's minimum dimension, i.e., $\kappa b \gg 1$, but the effect of double-layer relaxation is incorporated. The interaction between the solute ions and the charged surface of the cylinder is dominated by the electrical energies $\Phi_m = ez_m\Phi_e$, where z_m is the valence of ions m ($m = 1$ or 2; $-z_1 = z_2 = Z$) and Φ_e is the electrical potential.

Because n^∞ is not uniform, it is required that the total fluxes of cations and anions are equal in order to have no current arising from the diffusive fluxes of the solute ions in an electrically neutral solution. Thus, an electric field arises spontaneously due to the difference in mobilities of the cation and the anion [5],

$$\underset{\sim}{E}^\infty = -\nabla\Phi_e^\infty = \frac{kT}{Ze}\left(\frac{D_2 - D_1}{D_2 + D_1}\right)\nabla \ln n^\infty . \quad (39)$$

Since all the governing equations and boundary conditions are linear, diffusiophoresis can be considered a linear combination of two effects: 1) "chemiphoresis" due to the nonuniform adsorption of counterions over the surface of the particle, which is analogous to diffusiophoresis of nonelectrolytes considered in the previous section, and 2) "electrophoresis" due to the macroscopic electric field generated by the gradient of electrolyte concentration given by Eq. (39). In Eq. (3) for the diffusiophoretic velocity of a particle with an unpolarized double layer, the first term in the brackets results from the contribution of electrophoresis, while the other term represents the chemiphoretic contribution. Similar to the analysis in the previous section, here we can decompose ∇n^∞ into the transversal and longitudinal components, $(\nabla n^\infty)_x \underset{\sim}{e}_x + (\nabla n^\infty)_y \underset{\sim}{e}_y$ and $(\nabla n^\infty)_z \underset{\sim}{e}_z$, and analyze the diffusiophoretic motion due to each separately.

First, we consider the motion due to the transverse component. The modified chemical potentials (known as electrochemical potentials) of the ions outside the double layer satisfy the Laplace equation (12). A solution of them in terms of the elliptic cylinder coordinates that satisfies the far-field boundary condition (21) is

$$\mu_m = \mu_m^0 + kT \ln n^\infty(\underset{\sim}{0}) + \frac{kT(\nabla n^\infty)_x}{n^\infty(\underset{\sim}{0})} \times \left\{\left[1 - \frac{z_m}{Z}\left(\frac{D_2 - D_1}{D_2 + D_1}\right)\right] x + A_m e^{-\xi}\cos\varphi\right\} + \frac{kT(\nabla n^\infty)_y}{n^\infty(\underset{\sim}{0})}\left\{\left[1 - \frac{z_m}{Z}\left(\frac{D_2 - D_1}{D_2 + D_1}\right)\right] y + B_m e^{-\xi}\sin\varphi\right\}, \quad (40)$$

where $m = 1$ or 2, and A_1, A_2, B_1, and B_2 are unknown constants to be determined by using the boundary condition at the particle surface. In addition to the direct contribution of the solute gradient to μ_m, as is given by Eq. (25), a part due to the induced electric field given by Eq. (39) is also included in Eq. (40).

At the outer edge of the double layer surrounding the particle, normal gradients of the electrochemical potentials occur as described in Eq. (16). Since the equilibrium electrical potential Φ_e^0 governed by the Poisson-Boltzmann equation has an analytical expression for a symmetric electrolyte (so do Φ_1^0 and Φ_2^0), the values of β_{mi} in Eq. (18)

can be analytically determined [10],

$$\beta_{11} = \frac{1}{\kappa}\left[4\left(1 + \frac{3f_1}{Z^2}\right)\exp(\bar{\zeta})\sinh\bar{\zeta} - \frac{12f_1}{Z^2}(\bar{\zeta} + \ln\cosh\bar{\zeta})\right], \tag{41a}$$

$$\beta_{12} = \frac{-1}{\kappa}\left(\frac{12f_1}{Z^2}\right)\ln\cosh\bar{\zeta}, \tag{41b}$$

$$\beta_{21} = \frac{-1}{\kappa}\left(\frac{12f_2}{Z^2}\right)\ln\cosh\bar{\zeta}, \tag{41c}$$

$$\beta_{22} = \frac{1}{\kappa}\left[-4\left(1 + \frac{3f_2}{Z^2}\right)\exp(-\bar{\zeta})\sinh\bar{\zeta} + \frac{12f_2}{Z^2}(\bar{\zeta} - \ln\cosh\bar{\zeta})\right], \tag{41d}$$

where $\bar{\zeta} = Ze\zeta/4kT$ and $f_m = \varepsilon(kT)^2/6\pi\eta e^2 D_m$.

Substituting Eq. (40) into Eqs. (16), it is found that

$$A_1 = ce^{\xi_0}\frac{g_3g_5 - g_2g_6}{g_1g_5 - g_2g_4}, \tag{42a}$$

$$A_2 = ce^{\xi_0}\frac{g_1g_6 - g_3g_4}{g_1g_5 - g_2g_4}, \tag{42b}$$

$$B_1 = ce^{\xi_0}\frac{h_3h_5 - h_2h_6}{h_1h_5 - h_2h_4}, \tag{42c}$$

$$B_2 = ce^{\xi_0}\frac{h_1h_6 - h_3h_4}{h_1h_5 - h_2h_4}, \tag{42d}$$

where

$$\begin{Bmatrix} g_1 \\ h_1 \end{Bmatrix} = \frac{\pi}{2} + \frac{\beta_{11}}{c}\begin{Bmatrix} G(\xi_0) \\ H(\xi_0) \end{Bmatrix}, \tag{43a}$$

$$\begin{Bmatrix} g_2 \\ h_2 \end{Bmatrix} = \frac{\beta_{12}}{c}\begin{Bmatrix} G(\xi_0) \\ H(\xi_0) \end{Bmatrix}, \tag{43b}$$

$$\begin{Bmatrix} g_3 \\ h_3 \end{Bmatrix} = \frac{\pi D_2}{D_2 + D_1}\begin{Bmatrix} \sinh\xi_0 \\ \cosh\xi_0 \end{Bmatrix} - \frac{2(\beta_{11}D_2 + \beta_{12}D_1)}{c(D_2 + D_1)}\begin{Bmatrix} \cosh\xi_0\, G(\xi_0) \\ \sinh\xi_0\, H(\xi_0) \end{Bmatrix}, \tag{43c}$$

$$\begin{Bmatrix} g_4 \\ h_4 \end{Bmatrix} = \frac{\beta_{21}}{c}\begin{Bmatrix} G(\xi_0) \\ H(\xi_0) \end{Bmatrix}, \tag{43d}$$

$$\begin{Bmatrix} g_5 \\ h_5 \end{Bmatrix} = \frac{\pi}{2} + \frac{\beta_{22}}{c}\begin{Bmatrix} G(\xi_0) \\ H(\xi_0) \end{Bmatrix}, \tag{43e}$$

$$\begin{Bmatrix} g_6 \\ h_6 \end{Bmatrix} = \frac{\pi D_1}{D_2 + D_1}\begin{Bmatrix} \sinh\xi_0 \\ \cosh\xi_0 \end{Bmatrix} - \frac{2(\beta_{21}D_2 + \beta_{22}D_1)}{c(D_2 + D_1)}\begin{Bmatrix} \cosh\xi_0\, G(\xi_0) \\ \sinh\xi_0\, H(\xi_0) \end{Bmatrix}. \tag{43f}$$

In Eqs. (43), $G(\xi_0)$ and $H(\xi_0)$ are defined by Eqs. (30).

The fluid flow field outside the double layer is governed by the same equations as Eqs. (13) and (14) and obeys Eq. (32b). The boundary condition at the particle surface is, similar to Eq. (32a),

$$\xi = \xi_0^+ : \underline{v} = U_x\underline{e}_x + U_y\underline{e}_y - \underline{e}_\varphi\frac{1}{\eta c}(\sinh^2\xi + \sin^2\varphi)^{-\frac{1}{2}} \times \sum_{m=1}^{2}\frac{\partial\mu_m}{\partial\varphi}\int_0^\infty y_n[n_m^0 - n^\infty(\underline{0})]\,dy_n. \tag{44}$$

For a symmetric electrolyte, the integral in Eq. (44) can be analytically computed. Hence, the components of the diffusiophoretic velocity can be determined by a similar way to obtain Eqs. (34), with the result

$$U_x = \frac{\varepsilon\zeta}{4\pi\eta}\frac{kT}{Ze}\frac{(\nabla n^\infty)_x}{n^\infty(\underline{0})}\left[\frac{D_2 - D_1}{D_2 + D_1}e^{-\xi_0}\cosh\xi_0 + \frac{A_1 - A_2}{2c}e^{-2\xi_0} + \frac{4kT}{Ze\zeta}\ln\cosh\left(\frac{Ze\zeta}{4kT}\right) \times\left(e^{-\xi_0}\cosh\xi_0 + \frac{A_1 + A_2}{2c}e^{-2\xi_0}\right)\right], \tag{45a}$$

and

$$U_y = \frac{\varepsilon\zeta}{4\pi\eta}\frac{kT}{Ze}\frac{(\nabla n^\infty)_y}{n^\infty(\underline{0})}\left[\frac{D_2 - D_1}{D_2 + D_1}e^{-\xi_0}\sinh\xi_0 + \frac{B_1 - B_2}{2c}e^{-2\xi_0} + \frac{4kT}{Ze\zeta}\ln\cosh\left(\frac{Ze\zeta}{4kT}\right) \times\left(e^{-\xi_0}\sinh\xi_0 + \frac{B_1 + B_2}{2c}e^{-2\xi_0}\right)\right], \tag{45b}$$

The stream function for the fluid flow can still be expressed by Eq. (33), but here U_x and U_y are given by the above equations instead. Note that, in the limit of large κb and small $|\zeta|$ as expressed by Eq. (8), $\beta_{11}/b = \beta_{12}/b = \beta_{21}/b = \beta_{22}/b = 0$ and Eqs. (45) reduce to the form of Eq. (3) for the case of a thin unpolarized double layer. As expected, Eqs. (45) predict that $U_x = U_y = 0$ if $\zeta = 0$.

Due to the linearity of the diffusiophoretic problem, the particle velocities U_x and U_y can be expressed as

$$U_x = U_x^c + U_x^e \tag{46a}$$

and

$$U_y = U_y^c + U_y^e, \tag{46b}$$

where U_x^c and U_y^c represent the corresponding chemiphoretic velocities, and U_x^e and U_y^e denote the corresponding electrophoretic velocities. U_x^c and U_y^c can be determined from the same procedure to obtain Eq. (45) by setting $D_2 = D_1$ in Eq. (40) for μ_m,

$$U_x^c = \frac{\varepsilon\zeta}{4\pi\eta}\frac{kT}{Ze}\frac{(\nabla n^\infty)_x}{n^\infty(\mathrm{Q})}\left[\frac{A_1' - A_2'}{2c}e^{-2\xi_0} + \frac{4kT}{Ze\zeta}\ln\cosh\left(\frac{Ze\zeta}{4kT}\right)\times\left(e^{-\xi_0}\cosh\xi_0 + \frac{A_1' + A_2'}{2c}e^{-2\xi_0}\right)\right] \tag{47a}$$

and

$$U_y^c = \frac{\varepsilon\zeta}{4\pi\eta}\frac{kT}{Ze}\frac{(\nabla n^\infty)_y}{n^\infty(\mathrm{Q})}\left[\frac{B_1' - B_2'}{2c}e^{-2\xi_0} + \frac{4kT}{Ze\zeta}\ln\cosh\left(\frac{Ze\zeta}{4kT}\right)\times\left(e^{-\xi_0}\sinh\xi_0 + \frac{B_1' + B_2'}{2c}e^{-2\xi_0}\right)\right]. \tag{47b}$$

Here

$$A_1' = ce^{\xi_0}\frac{g_3'g_5 - g_2g_6'}{g_1g_5 - g_2g_4}, \tag{48a}$$

$$A_2' = ce^{\xi_0}\frac{g_1g_6' - g_3'g_4}{g_1g_5 - g_2g_4}, \tag{48b}$$

$$B_1' = ce^{\xi_0}\frac{h_3'h_5 - h_2h_6'}{h_1h_5 - h_2h_4}, \tag{48c}$$

$$B_2' = ce^{\xi_0}\frac{h_1h_6' - h_3'h_4}{h_1h_5 - h_2h_4}, \tag{48d}$$

where

$$\begin{Bmatrix} g_3' \\ h_3' \end{Bmatrix} = \frac{\pi}{2}\begin{Bmatrix} \sinh\xi_0 \\ \cosh\xi_0 \end{Bmatrix} - \frac{\beta_{11} + \beta_{12}}{c}\begin{Bmatrix} \cosh\xi_0\, G(\xi_0) \\ \sinh\xi_0\, H(\xi_0) \end{Bmatrix}, \tag{49a}$$

$$\begin{Bmatrix} g_6' \\ h_6' \end{Bmatrix} = \frac{\pi}{2}\begin{Bmatrix} \sinh\xi_0 \\ \cosh\xi_0 \end{Bmatrix} - \frac{\beta_{21} + \beta_{22}}{c}\begin{Bmatrix} \cosh\xi_0\, G(\xi_0) \\ \sinh\xi_0\, H(\xi_0) \end{Bmatrix}. \tag{49b}$$

In the limit of Eq. (8), Eqs. (47) reduce to Eq. (3) with $D_2 = D_1$.

On the other hand, U_x^e and U_y^e can be determined similarly by eliminating the first terms in the square brackets in Eq. (40),

$$U_x^e = \frac{\varepsilon\zeta}{4\pi\eta}\frac{kT}{Ze}\frac{(\nabla n^\infty)_x}{n^\infty(\mathrm{Q})}\frac{D_2 - D_1}{D_2 + D_1}\left[e^{-\xi_0}\cosh\xi_0 + \frac{A_1'' + A_2''}{2c}e^{-2\xi_0} + \frac{4kT}{Ze\zeta}\ln\cosh\left(\frac{Ze\zeta}{4kT}\right)\times\frac{A_1'' - A_2''}{2c}e^{-2\xi_0}\right] \tag{50a}$$

and

$$U_y^e = \frac{\varepsilon\zeta}{4\pi\eta}\frac{kT}{Ze}\frac{(\nabla n^\infty)_y}{n^\infty(\mathrm{Q})}\frac{D_2 - D_1}{D_2 + D_1}\left[e^{-\xi_0}\sinh\xi_0 + \frac{B_1'' + B_2''}{2c}e^{-2\xi_0} + \frac{4kT}{Ze\zeta}\ln\cosh\left(\frac{Ze\zeta}{4kT}\right)\times\frac{B_1'' - B_2''}{2c}e^{-2\xi_0}\right]. \tag{50b}$$

Here,

$$A_1'' = ce^{\xi_0}\frac{g_3''g_5 - g_2g_6''}{g_1g_5 - g_2g_4}, \tag{51a}$$

$$A_2'' = -ce^{\xi_0}\frac{g_1g_6'' - g_3''g_4}{g_1g_5 - g_2g_4}, \tag{51b}$$

$$B_1'' = ce^{\xi_0}\frac{h_3''h_5 - h_2h_6''}{h_1h_5 - h_2h_4}, \tag{51c}$$

Table 2. The normalized diffusiophoretic mobilities of an elliptic cylinder in a solution containing only one symmetric electrolyte with $Z = 1$, $f_1 = 0.2$, and $\zeta e/kT = 8$ in the transverse directions parallel to the major axis (x) and the minor axis (y)

κa	κb	$a/b = 1.1$		$a/b = 1.01$		$a/b = 1$
		U_x/U_{x0}	U_y/U_{y0}	U_x/U_{x0}	U_y/U_{y0}	U/U_0
			$(D_2 - D_1)/(D_2 + D_1) = 0$			
100		0.2230	0.2092	0.2291	0.2276	0.2298
	100	0.2513	0.2371	0.2320	0.2305	
300		0.5564	0.5428	0.5623	0.5609	0.5630
	300	0.5832	0.5699	0.5651	0.5637	
1000		0.8225	0.8152	0.8256	0.8249	0.8260
	1000	0.8365	0.8297	0.8271	0.8264	
			$(D_2 - D_1)/(D_2 + D_1) = -0.2$			
100		0.1154	0.0995	0.1222	0.1206	0.1231
	100	0.1476	0.1314	0.1256	0.1239	
300		0.4953	0.4749	0.5019	0.5003	0.5027
	300	0.5258	0.5107	0.5051	0.5035	
1000		0.7981	0.7897	0.8016	0.8008	0.8021
	1000	0.8140	0.8062	0.8033	0.8025	

$$B_2'' = -ce^{\xi_0}\frac{h_1 h_6'' - h_3'' h_4}{h_1 h_5 - h_2 h_4}, \tag{51d}$$

where

$$\begin{Bmatrix} g_3'' \\ h_3'' \end{Bmatrix} = \frac{\pi}{2}\begin{Bmatrix} \sinh\xi_0 \\ \cosh\xi_0 \end{Bmatrix} - \frac{\beta_{11} - \beta_{12}}{c}\begin{Bmatrix} \cosh\xi_0\, G(\xi_0) \\ \sinh\xi_0\, H(\xi_0) \end{Bmatrix}, \tag{52a}$$

$$\begin{Bmatrix} g_6'' \\ h_6'' \end{Bmatrix} = -\frac{\pi}{2}\begin{Bmatrix} \sinh\xi_0 \\ \cosh\xi_0 \end{Bmatrix} - \frac{\beta_{21} - \beta_{22}}{c} \times \begin{Bmatrix} \cosh\xi_0\, G(\xi_0) \\ \sinh\xi_0\, H(\xi_0) \end{Bmatrix}. \tag{52b}$$

For the motion driven by the longitudinal component $(\nabla n^\infty)_z$ of the solute gradient, no polarization of the diffuse ions or disturbance in the fluid velocity and solute concentration fields arises. The diffusiophoretic velocity of the cylinder is the same as that predicted by Eq. (3),

$$U_z = \frac{\varepsilon\zeta}{4\pi\eta}\frac{kT}{Ze}\frac{(\nabla n^\infty)_z}{n^\infty(\infty)}\left[\frac{D_2 - D_1}{D_2 + D_1} + \frac{4kT}{Ze\zeta}\ln\cosh\left(\frac{Ze\zeta}{4kT}\right)\right]. \tag{53}$$

The overall diffusiophoretic velocity of an arbitrarily oriented elliptic cylinder and the ensemble-averaged mobility of the elliptic cylinder can also be determined by Eqs. (36) and (37), respectively, incorporated with Eqs. (45) and (53).

The coefficients A_1, A_2, B_1, and B_2 in Eq. (45) have been calculated for various values of $(D_2 - D_1)/(D_2 + D_1)$, f_1, Z, $\zeta e/kT$, κa, and a/b. Part of the numerical results of the diffusiophoretic velocities U_x and U_y of the elliptic cylinder (with $Z = 1$, $f_1 = 0.2$, $\zeta e/kT = 8$, $a/b = 1.1$ and 1.01) normalized by their corresponding magnitudes (U_{x0} and U_{y0}) with negligible effect of the double-layer polarization are presented in Table 2. The analytical solutions of the diffusiophoretic velocity of a circular cylinder as given by Eq. (10) are also listed in the last column of this table for comparison. It can be seen that the results for the elliptic cylinder agree very well in trend with the exact values for the circular cylinder. The diffusiophoretic mobilities are always reduced due to the polarization of the double layer. Also, the normalized velocity U_x/U_{x0} is a much less sensitive function of the aspect ratio a/b for a given value of κa than for a given value of κb, while U_y/U_{y0} is a much less sensitive function of a/b for a fixed κb than for a fixed κa. Similarly to the case of diffusiophoresis of an elliptic cylinder in nonelectrolytes considered in the previous section, the diffusiophoretic velocity of a cylinder in electrolytes decreases with the reduction of the maximum

length of the particle in the direction of diffusiophoresis. Note that the situations associated with $(D_2 - D_1)/(D_2 + D_1) = 0$ and -0.2 in Table 2 are very close to the diffusiophoresis in the aqueous solutions of KCl and NaCl, respectively.

In Figs. 4a–c, the dependence of the average diffusiophoretic velocity in a dilute dispersion of identical elliptic cylinders on their dimensionless zeta potential at various values of a/b and Z for a case that the anion and cation mobilities are equal ($D_2 - D_1 = 0$ with $f_1 = f_2 = 0.2$ and $\kappa a = 300$) is illustrated. Here, the magnitude of the diffusiophoretic velocity is normalized by a characteristic value

$$U^* = \frac{\varepsilon}{4\pi\eta}\left(\frac{kT}{e}\right)^2 \frac{|\nabla n^\infty|}{n^\infty(0)}. \tag{54}$$

Only the results at positive zeta potentials are shown in Figs. 4a–c since the induced electric field given by Eq. (39) disappears for $D_2 = D_1$ and the diffusiophoretic velocity, which is due to the chemiphoretic effect only, is an even function of zeta potential. It can be seen from Figs. 4b and 4c that the diffusiophoretic velocity does not vary monotonically with the zeta potential of the particles, and a local maximum and a local minimum in the average mobility occur at some values of $\zeta e/kT$ which depend on a/b and Z. When a/b or Z increases, the local maximum or minimum will take place at a smaller magnitude of zeta potential (for a fixed value of κa). Note that the upward trend of the average diffusiophoretic mobility for large zeta potentials in Figs. 4b and 4c results from the contribution of the particle mobility in the axial direction, in which the polarization effect of the double layer does not appear.

Figures 5a–c are drawn for the normalized average diffusiophoretic velocity in a dilute dispersion of identical elliptic cylinders as a function of $\zeta e/kT$ at various values of a/b and Z for a case that the anion and cation have different diffusion coefficients ($(D_2 - D_1)/(D_2 + D_1) = -0.2$ with $f_1 = 0.2$ and $\kappa a = 300$). In this case, both the chemiphoretic and the electrophoretic effects contribute to the particles' movement and the net diffusiophoretic velocity is neither an even nor an odd function of ζ. The curves in Figs. 5a–c show that the average diffusiophoretic velocity might reverse direction six times as the zeta potential of the particles varies from highly negative to highly

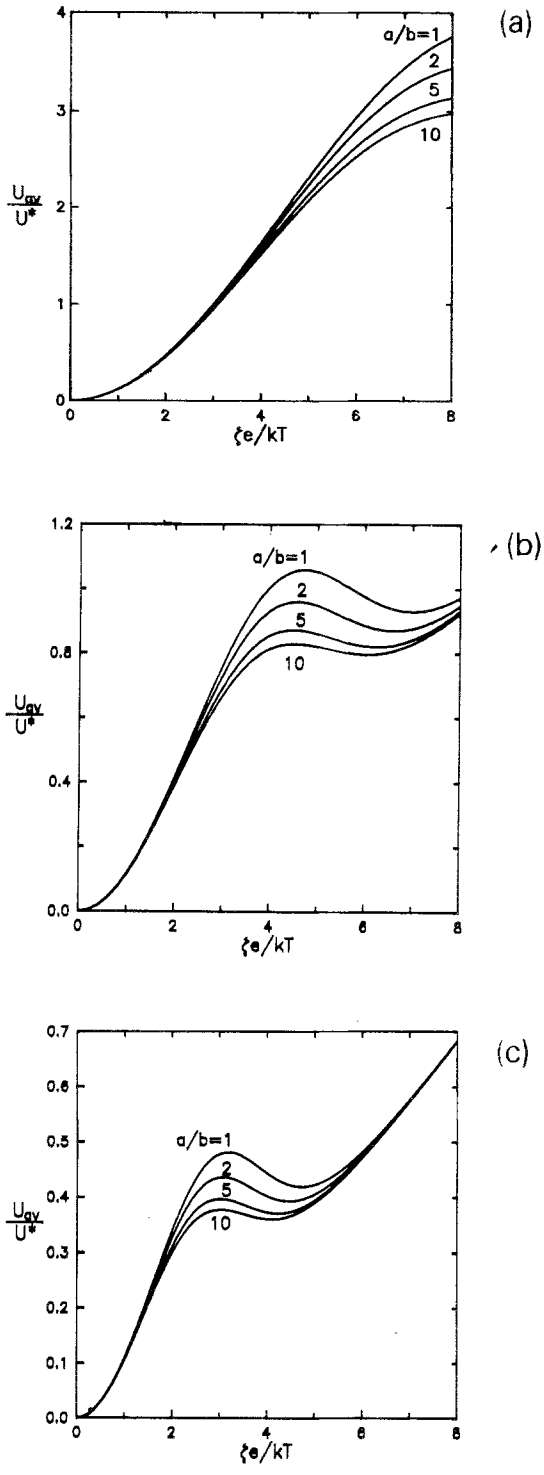

Fig. 4. Plots of the normalized average diffusiophoretic mobility in a dilute suspension of identical elliptic cylinders with a symmetric-electrolyte concentration gradient versus the dimensionless zeta potential of the particles for various values of the aspect ratio a/b with $D_1 - D_2 = 0$, $f_1 = f_2 = 0.2$ and $\kappa a = 300$: a) $Z = 1$; b) $Z = 2$; c) $Z = 3$

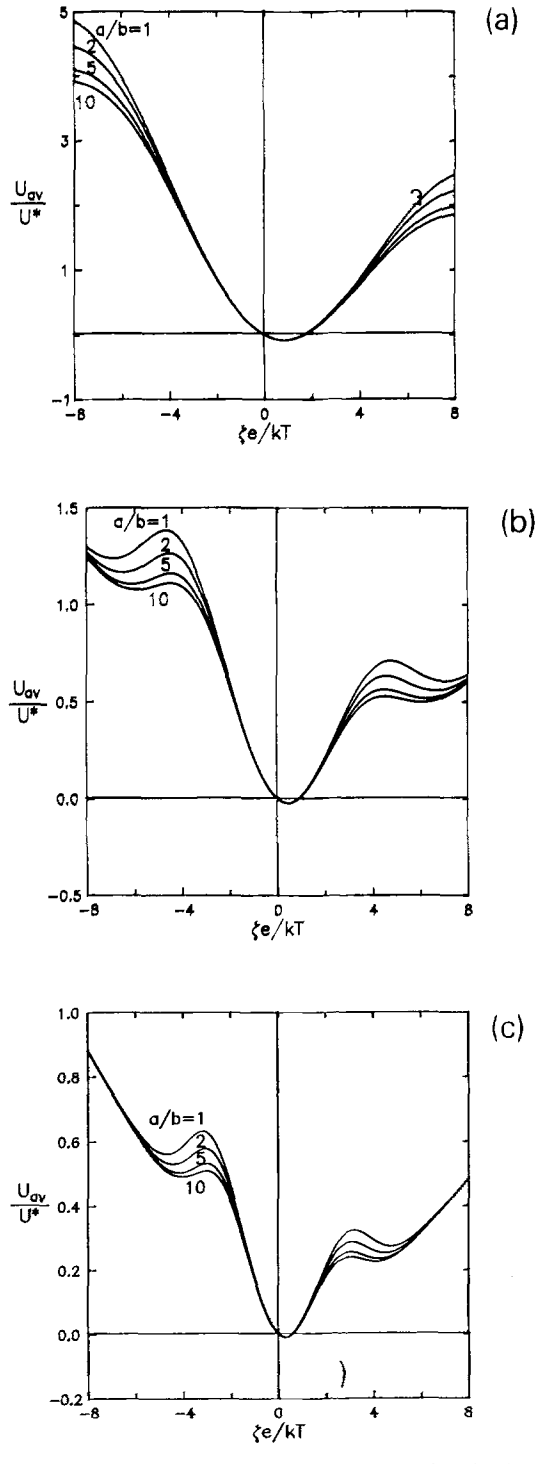

Fig. 5. Plots of the normalized average diffusiophoretic mobility in a dilute suspension of identical elliptic cylinders with a symmetric-electrolyte concentration gradient versus the dimensionless zeta potential of the particles for various values of the aspect ratio a/b with $(D_2 - D_1)/(D_2 + D_1) = -0.2$, $f_1 = 0.2$ and $\kappa a = 300$: a) $Z = 1$; b) $Z = 2$; c) $Z = 3$

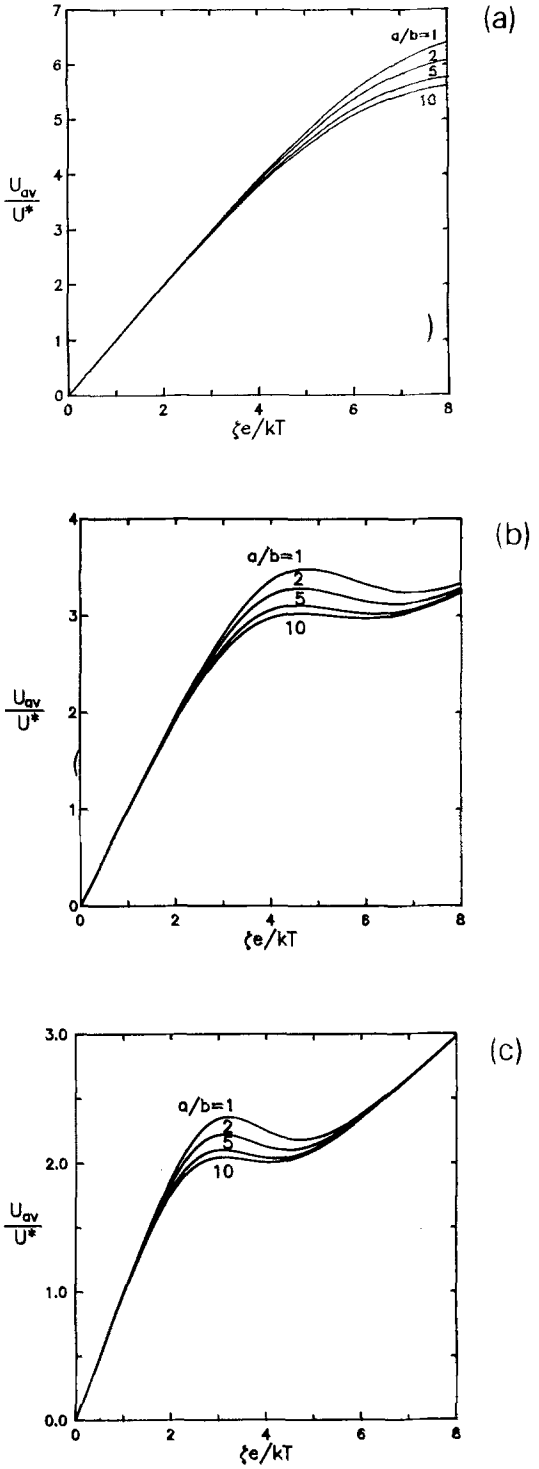

Fig. 6. Plots of the normalized average electrophoretic mobility in a dilute suspension of identical elliptic cylinders with a symmetric electrolyte in the solution versus the dimensionless zeta potential of the particles for various values of the aspect ratio a/b with $f_1 = f_2 = 0.2$ and $\kappa a = 300$: a) $Z = 1$; b) $Z = 2$; c) $Z = 3$

positive values. Similarly to Figs. 4b and 4c for the case of $D_2 = D_1$, the upward trend of the average diffusiophoretic mobility at large magnitudes of zeta potential illustrated in Figs. 5b and 5c is due to the contribution of the particle mobility in the axial direction. It can be seen from Figs. 4 and 5 and Table 2 that the normalized particle velocities are monotonic decreasing functions of a/b for a fixed value of κa and are monotonic increasing functions of a/b for a given value of κb.

5. Electrophoresis in symmetric electrolytes

Considered in this section is the electrophoretic motion of a charged elliptic cylinder when a uniform external electric field $\underset{\sim}{E}^{\infty}$ is imposed. The bulk concentrations of all ions n_m^{∞} beyond the electrical double layer are constant. The thickness of the double layer is assumed to be much smaller than the minimum particle dimension ($\kappa b \gg 1$). The potential energy Φ_m of ionic species m is equal to $ez_m\Phi_e$. Like the analysis in the previous sections, the imposed electric field can be vectorially decomposed into the longitudinal component $E_z^{\infty}\underset{\sim}{e}_z$ and the transversal component $E_x^{\infty}\underset{\sim}{e}_x + E_y^{\infty}\underset{\sim}{e}_y$. For simplicity, only one symmetric electrolyte in the liquid phase ($M = 2$; $-z_1 = z_2 = Z$; $n_1^{\infty} = n_2^{\infty} = n^{\infty}$, where subscripts 1 and 2 denote anion and cation respectively) will be considered.

First, we examine the motion due to $E_x^{\infty}\underset{\sim}{e}_x + E_y^{\infty}\underset{\sim}{e}_y$. Outside the double layer, the electrochemical potentials, which satisfy Laplace's equation (12), can be expressed as

$$\mu_m = \mu_m^0 + kT\ln n^{\infty}(\underset{\sim}{0}) - ez_mE_x^{\infty}[x + A_m''e^{-\xi}\cos\varphi] - ez_mE_y^{\infty}[y + B_m''e^{-\xi}\sin\varphi] , \tag{55}$$

where $m = 1$ or 2. This solution immediately satisfies the far-field condition, $\nabla\mu_m \to -ez_m(E_x^{\infty}\underset{\sim}{e}_x + E_y^{\infty}\underset{\sim}{e}_y)$ as $(x^2 + y^2)^{\frac{1}{2}} \to \infty$. At the outer edge of the double layer, normal fluxes of ions take place as described by Eq. (16). The parameters β_{mi} have been given in Eqs. (41). The unknown coefficients A_1'', A_2'', B_1'', and B_2'' in Eq. (55) can also be determined using Eqs. (51). Following the procedure in the previous section, we can find the components of the transverse electrophoretic velocity, with

$$U_x = \frac{\varepsilon\zeta}{4\pi\eta}E_x^{\infty}\left[e^{-\xi_0}\cosh\xi_0 + \frac{A_1'' + A_2''}{2c}e^{-2\xi_0} + \frac{4kT}{Ze\zeta}\ln\cosh\left(\frac{Ze\zeta}{4kT}\right)\frac{A_1'' - A_2''}{2c}e^{-2\xi_0}\right] \tag{56a}$$

and

$$U_y = \frac{\varepsilon\zeta}{4\pi\eta}E_y^{\infty}\left[e^{-\xi_0}\sinh\xi_0 + \frac{B_1'' + B_2''}{2c}e^{-2\xi_0} + \frac{4kT}{Ze\zeta}\ln\cosh\left(\frac{Ze\zeta}{4kT}\right)\frac{B_1'' - B_2''}{2c}e^{-2\xi_0}\right] . \tag{56b}$$

These expressions can also be obtained from Eqs. (50) with the substitution of Eq. (39). When κb is large and $|\zeta|$ is small such that Eq. (8) is satisfied, Eqs. (56) reduce to Smoluchowski's equation. The stream function for the fluid flow here is also provided by Eq. (33) with U_x and U_y given by Eqs. (56).

Because there is no polarization of the diffuse ions near the cylinder surface in an electric field parallel to its axis, the longitudinal component of the particle velocity is what the Smoluchowski equation predicts,

$$U_z = \frac{\varepsilon\zeta}{4\pi\eta}E_z^{\infty} . \tag{57}$$

The total electrophoretic velocity and the ensemble-averaged mobility of the elliptic cylinder can also be determined by Eqs. (36) and (37), with $(\nabla n^{\infty})_x$, $(\nabla n^{\infty})_y$, $(\nabla n^{\infty})_z$, and ∇n^{∞} in Eq. (37) being replaced by E_x^{∞}, E_y^{∞}, E_z^{∞} and $\underset{\sim}{E}^{\infty}$, respectively.

The coefficients A_1'', A_2'', B_1'', and B_2'' in Eqs. (56) have been calculated for various values of Z, $\zeta e/kT$, κa, and a/b. Part of the numerical results of the electrophoretic velocities of the elliptic cylinder (with $Z = 1$, $f_1 = f_2 = 0.2$, $\zeta e/kT = 8$, $a/b = 1.1$ and 1.01) normalized by their corresponding magnitudes with negligible relaxation effect of the double layer are listed in Table 3. The exact solutions of the electrophoretic velocity of a circular cylinder calculated using Eq. (5) are also given in the last column of this table for comparison. Again, the results for the elliptic cylinder can be found to agree very well in trend with the analytical solutions for the circular cylinder.

Table 3. The normalized electrophoretic mobilities of an elliptic cylinder in a solution containing only one symmetric electrolyte with $Z = 1$, $f_1 = f_2 = 0.2$, and $\zeta e/kT = 8$ in the transverse directions parallel to the major axis (x) and the minor axis (y)

κa	κb	$a/b = 1.1$		$a/b = 1.01$		$a/b = 1$
		U_x/U_{x0}	U_y/U_{y0}	U_x/U_{x0}	U_y/U_{y0}	U/U_0
100		0.4702	0.4609	0.4742	0.4732	0.4747
	100	0.4891	0.4796	0.4762	0.4752	
300		0.6963	0.6870	0.7003	0.6993	0.7008
	300	0.7146	0.7055	0.7022	0.7012	
1000		0.8783	0.8733	0.8804	0.8799	0.8807
	1000	0.8879	0.8832	0.8815	0.8810	

Similarly to the cases of diffusiophoresis considered in the previous sections, the electrophoretic mobilities are reduced due to the polarization of the double layer. These normalized mobilities are monotonic decreasing functions of a/b for a given value of κa and are monotonic increasing functions of a/b for a fixed value of κb. Also, the normalized electrophoretic velocity of an elliptic cylinder decreases with the reduction of the maximum length of the particle in the direction of migration. Only one case of the ionic mobilities is considered here since their influence on the electrophoretic velocity of particles is generally weak for most realistic aqueous systems [10].

The average electrophoretic velocity in a dilute suspension of identical elliptic cylinders as a function of $\zeta e/kT$ at various values of a/b and Z for the case with $f_1 = f_2 = 0.2$ and $\kappa a = 300$ is depicted in Figs. 6a–c. In these figures, the magnitude of this average velocity is normalized by the characteristic value

$$U^* = \frac{\varepsilon}{4\pi\eta}\left(\frac{kT}{e}\right)|\underline{E}^\infty| \,. \tag{58}$$

Only the results at positive zeta potentials are displayed in Figs. 6a–c since the electrophoretic velocity is an odd function of zeta potential for the situation that the anion and cation mobilities are equal. Similarly to the case of chemiphoresis as shown in Figs. 4b and 4c, the electrophoretic velocity does not vary monotonically with the zeta potential, and a local maximum and a local minimum in the particle mobility appear at some values of $\zeta e/kT$ which depend on a/b and Z. When a/b or Z increases, the local maximum or minimum for each value of κa will occur at a smaller magnitude of zeta potential. Also, Figs. 6b and 6c show the upward tendency of the average electrophoretic mobility of the cylinder at high zeta potentials.

6. Summary

Three problems of similar physical and mathematical structures are studied in this work: the diffusiophoresis of an elliptic cylinder in a nonelectrolyte solute gradient, the diffusiophoresis of an elliptic cylinder in an electrolyte solute gradient, and the electrophoresis of an elliptic cylinder in an external electric field. The cylinder can be oriented arbitrarily with respect to the applied field. Although the region of the interaction between the solute species and the particle surface is taken to be small relative to the particle dimension, the assumptions allow for polarization of the mobile species in the diffuse layer. The method developed for solving the electrokinetic equations in the limit of thin double layer [3, 9] has been used to solve the equations of conservation applicable to the problems.

Expressions for the diffusiophoretic and electrophoretic velocities of the elliptic cylinder were obtained in Eqs. (34), (45), and (56) for various transversal imposed fields and could be found in Eqs. (35), (53), and (57) for various longitudinal imposed fields. An important result that the particle velocity decreases with the reduction of the maximum length of the particle in the direction of migration was deduced. Although the validity of Eqs. (45) and (56) is restricted to the case of a

symmetric electrolyte solution, formulae for a fluid containing an arbitrary combination of general electrolytes can be obtained from the same procedure using O'Brien's [9] reasoning that only the most highly charged counterions play a dominant role in the ionic fluxes along the particle surface. Due to the linearity of these problems, the migration velocity of the cylinder in an arbitrarily oriented applied field can be obtained by the vectorial addition of the contributions generated from the transversal and longitudinal components of the applied field. The average diffusiophoretic or electrophoretic velocity for an ensemble of identical elliptic cylinders can also be calculated from the transversal and longitudinal mobilities of the particle. It has been found that the normalized phoretic velocities are monotonic decreasing functions of the aspect ratio a/b for a given value of the relaxation parameter β/a (or κa) and are monotonic increasing functions of a/b for a given value of β/a (or (κb).

Acknowledgment

This research was supported by the National Science Council of the Republic of China.

References

1. Anderson JL (1989) Ann Rev Fluid Mech 21:61–99
2. Morrison FA (1970) J Colloid Interface Sci 34:210–214
3. Dukhin SS, Derjaguin BV (1974) In: Matijević E (ed) Surface and Colloid Science Vol 7 Wiley, New York
4. Anderson JL, Lowell ME, Prieve DC (1982) J Fluid Mech 117: 107–121
5. Prieve DC, Anderson JL, Ebel JP, Lowell ME (1984) J Fluid Mech 148:247–269
6. O'Brien RW, White LR (1978) J Chem Soc Faraday Trans II 74:1607–1626
7. O'Brien RW, Hunter RJ (1981) Can J Chem 59:1878–1887
8. Ohshima H, Healy TW, White LR (1983) J Chem Soc Faraday Trans II 79:1613–1628
9. O'Brien RW (1983) J Colloid Interface Sci 92:204–216
10. Chen SB, Keh HJ (1992) J Fluid Mech 238:251–276
11. Anderson JL, Prieve DC (1991) Langmuir 7:403–406
12. Prieve DC, Roman R (1987) J Chem Soc Faraday Trans II 83:1287–1306
13. Keh HJ, Chen SB (1993) Langmuir 9:1142–1149
14. Stigter D (1978) J Phys Chem 82:1417–1423
15. Stigter D (1978) J Phys Chem 82:1424–1429
16. O'Brien RW, Ward DN (1988) J Colloid Interface Sci 121:402–413
17. Keh HJ, Huang TY (1993) J Colloid Interface Sci 160:354–371
18. Happel J, Brenner H (1983) Low Reynolds Number Hydrodynamics. Martinus Nijhoff, The Netherlands, pp 495–497
19. Spiegel MR (1968) Mathematical Handbook of Formulas and Tables. McGraw-Hill, New York, p 254
20. Lamb H (1932) Hydrodynamics, 6th ed. Cambridge Univ Press, Cambridge, pp 84–85

Received April 2, 1993;
accepted September 24, 1993

Authors' address:

Professor Huan J. Keh
Department of Chemical Engineering
National Taiwan University
Taipei 106–17 Taiwan
Republic of China